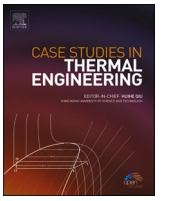
Case Studies in Thermal Engineering 49 (2023) 103145



Contents lists available at ScienceDirect

Case Studies in Thermal Engineering

journal homepage: www.elsevier.com/locate/csite



Artificial neural network models for heat transfer in the freeboard of a bubbling fluidised bed combustion system

Nimeti Doner [a,*], Kerem Ciddi [b], Ibrahim Berk Yalcin [a], Muhammed Sarivaz [a]

[a] Gazi University, Engineering Faculty, Mechanical Engineering Department, 06570, Ankara, Turkiye
[b] Kutahya Dumlupinar University, Industrial Engineering Department, 43270, Kutahya, Turkiye

ARTICLE INFO

Handling Editor: Dr Y Su

Keywords:
Fluidised bed
Artificial neural networks
Coal
Gas absorption
Heat transfer

ABSTRACT

The heat transfer in the combustion chamber (freeboard) of a fluidised bed combustor is of critical importance, due to the need for thermal efficiency, the possible environmental impacts, and the increasing costs of fuel and electricity. In this study, an artificial neural network model was used to analyse the heat transfer in a bubbling fluidised bed combustion system. The heat transfer of the system was investigated using temperature measurements of the combustion chamber and side wall of a 0.3 MWe fluidised bed combustor, the fly ash contents (%) of 40 types of coal, the gas absorption coefficients (CO_2 and H_2O vapour), and the enthalpy of the flue gas. The whole system was analysed using a backpropagation algorithm (10 hidden layers with 10 neurons). It was found that the most important factor when calculating the heat transfer in the combustion chamber was the height of the chamber, and the influence of the flue gas enthalpy and the ash particle content on the heat transfer accounted for 4% and 8.6%, respectively. The accuracy of the results from the proposed multilayer perceptron algorithm is high, and analyses could be performed for different values of the input data.

1. Introduction

Certain solid fuels burn rapidly and turbulently in fluidised bed combustor (FBC) systems under atmospheric or oxy-atmospheric conditions. The objective of a combustion system is to convert the chemical energy of the fuel into useful heat energy, by providing an adequate mixture of fuel and air. An FBC can use several types of fuel, such as low calorific value lignite, bituminous lignite, bituminous coal, petroleum coke, and biomass. Combustion occurs when air is supplied to a system with a mixture of fuels and bed materials (ash, lime, sand) in the combustion chamber. High thermal efficiency is achieved by a coal-gas mixture, and volatile particles are processed in the FBC over a long period of time [1]. The gases produced during combustion, such as CO_2, CO, nitrogen oxides (NOx) and sulphur dioxide (SO_2), cause air pollution, and the conditions in the combustion chambers are controlled due to their impact on climate change, as it is important that these gases are not released into the air.

The combustion air in an FBC is supplied via the bottom and side nozzles, and the bed temperature is 800–900 °C. The air supplied from the bottom (known as primary air) provides fluidity, while the air supplied from the sides (also called combustion air) ensures the efficiency of the combustion process of the fuel in the combustion chamber. When coal particles are thrown up the furnace, a fluidisation process takes place as they are mixed with the limestone. The primary air is supplied at high pressure to keep the coal particles suspended in the air in the combustion environment, and coal firing occurs in this suspended state. Particles consisting of partially

* Corresponding author.
E-mail address: nimetidoner@gazi.edu.tr (N. Doner).

https://doi.org/10.1016/j.csite.2023.103145
Received 17 February 2023; Received in revised form 20 April 2023; Accepted 31 May 2023
Available online 12 June 2023
2214-157X/© 2023 The Authors. Published by Elsevier Ltd. This is an open access article under the CC BY-NC-ND license (http://creativecommons.org/licenses/by-nc-nd/4.0/).

burned coal, limestone and ash are carried by the flue gases to the upper part of the furnace, where combustion is fully achieved with combustion air [2]. FBC systems can generally be divided into two types: one relies on bubbling (BFBC), and the other on circulating (CFBC). The mixture of fuel, air, fly ash and volatiles from the combustion products in the combustion chamber of a BFBC gives off heat to the water tubes located at the top of the furnace. The particles from the combustion chamber are separated according to their size, in so-called cyclones, and the larger particles are returned to the combustion chamber [3,4]. A CFBC involves small particles (<1 mm) and high gas velocities [5]; in BFBC systems, the particle size distributions are larger and the gas velocity is lower, as the size of the particles in the combustion chamber is 0.1–4 mm and the gas velocity is designed for minimum mass transport.

Artificial neural networks (ANNs) have been successfully used for modelling, classifying, correlating, and interpreting variables using evolving computer technology [6]. For example, coal combustion performance has been analysed by Zhou et al. using an ANN model based on parameters such as NOx gas emissions, excess air ratio, coal properties, boiler load, and burner position and inclination [7]. The authors attempted to determine appropriate combustion conditions for reducing NOx emissions and unburned carbon in ash in a pulverised coal combustion system by using a multipurpose genetic program together with an ANN model. It is well known that pulverised coal combustion is different from fluidised bed combustion. Chandok, Kar and Tuli [8] studied the furnace exit temperatures in two-pass FBC systems using a backpropagation algorithm with an ANN model, and showed that this method could be applied to a combustion system of 210 MW for furnace optimisation. Krzywanski and Nowak [9] analysed the total heat transfer coefficients of the combustion chamber walls as a function of the operating parameters of a 260 MWe FBC using an ANN model. The cross-sectional area of the bottom of the combustion chamber was 21.2 × 5.2 m, and its height was 48 m. The wall heat transfer coefficients were determined with an error of less than 4%. Li et al. [10] investigated the etching properties of coal ash from a FBC using an ANN model, and their experimental results were confirmed by modelling based on the combustion ashes from the upper furnace of a 550 MWe FBC system (with length, width, and height 39.6 × 10.8 × 52 m). The combustion events in a CFBC were analysed using two algorithms (personally generated networks and k-means clustering) for flue gas emissions, corresponding to low and high load conditions of the furnace [11]. The authors performed effective and useful analyses with an ANN method using a dataset containing 10,000 samples of 46 types. To detect the effects of particles in a CFBC system, the system was analysed using two types of ANN model [12]. In another study, NOx and SO_2 gas emissions from FBC systems were analysed using an ANN-based machine learning method (ELM) [13]. Serrano and Castello [14] studied tar formation in a gasification system with a BFBC using one- and two-layer feedforward algorithms based on an ANN model. The characteristics of the co-combustion of coal gangue and peanut shells in an air atmosphere were studied experimentally and numerically using an ANN [15]. In these analyses, it was found that the defining characteristics of the input and output datasets strongly influenced the results.

Heat transfer in a combustion chamber depends on a variety of very different parameters, such as the temperature distribution of the medium, the particle load in the medium (particle size distribution, content), the radiative properties of the gases in the combustion chamber (complex refractive index, wavelength) and the geometry of the combustor (cylindrical or cartesian geometry, length). Without going into the mathematical formulations and calculation details of these parameters, we use an ANN model to identify the parameters affecting the heat transfer of a BFBC. This should make it easier to analyse the design and performance of such systems. To the best of our knowledge, the literature does not contain studies of the effects of the medium temperature, the gas absorption properties (CO_2 and H_2O vapour), the percentages of the fly ash components and the enthalpy of the flue gas, which affect the heat transfer in a BFBC system, on the heat transfer in a combustion chamber. We therefore apply an ANN model to a BFBC system to examine both the effects of these variables on the heat transfer performance of the system and their relationships to each other.

2. Structure of the ANN

The creation of an ANN consists of two phases: the first is the training phase, and the second involves evaluation and test procedures. The selection of the datasets used in these phases is very important. This approach is used to solve complex nonlinear problems to improve and increase productivity, using an archived dataset for each process. The experimental dataset and the results of the problem are defined as the inputs and outputs of the program to form a learning process. This method may involve different learning algorithms, such as single and multilayer feedforward networks, feedback networks, the Levenberg-Marquardt (LM) algorithm, scaled combined gradient (SCG), conjugate gradient backpropagation, momentum backpropagation, steepest descent backpropagation, quasi-Newton algorithms and self-constructed networks. The relationships between neurons are evaluated using hidden layers between the input and output datasets [16,17]. Of these algorithms, LM provides the most stable and fastest solution, and uses a combination of two minimisation methods (gradient reduction and the Gauss-Newton method). In an ANN analysis, each run is a learning process in which the weights of the neurons are changed according to the chosen learning method, and this is repeated until convergence is achieved for each learning process. ANNs are used for improvement and analysis in many different fields of engineering, such as product analysis in coal liquefaction [18], the evaluation of polycyclic aromatic hydrocarbons (PAH) and particulate emissions from diesel engines as a function of the fuel parameters and operating conditions [19,20], and the calculation of the specific heat of hybrid nanofluids [21].

An ANN consists of three types of layers, known as input, hidden, and output layers. The input data always flow from the input layer, and are transferred to the output layer by renewal of the learning-training rule using activation functions, weights ($\boldsymbol{w}$), and prediction vectors ($\boldsymbol{b}$) between neurons in the hidden layers. In studies using ANN models, different percentages of the dataset have been used for training, evaluation, and testing; however, in general, 70% of the data are used for training, 15% for evaluation, and 15% for testing, and these data are randomly selected. When modelling using an ANN with hidden layers, the tansig (tangent sigmoid function) and logsig (logarithmic sigmoid function) comparison criteria given in Eq. (1) are used, and a linear function expression (purelin) is used for the output layer [11,22].

$$\text{tansig}\, f(x) = (e^{x} - e^{-x}) \Big/ (e^{x} + e^{-x}), \quad \text{logsig}\, f(x) = \frac{1}{(1 + e^{-x})} \tag{1}$$

Here, x represents the vector (i.e., data) transmitted by the first layer. When applying this method, a term representing the root mean square error (Eq. (2)) between the target values and the computed values is applied in each learning process.

$$E = \sqrt{\frac{1}{q} \sum_{s=1}^{q} \left(y_s - y_{s,t}\right)^2} \tag{2}$$

where E is the square root of the mean total error, y_s is the initial value of the method for the training example s, $y_{s,t}$ is the target initial value from the experimental results, and q is the number of learning samples. The input data have important effects on the process under consideration, and their selection is very important when applying this model. The selection of the target data is also very important for the purposes of the study. The training, evaluation and test results are expressed in terms of an R value, which is called the correlation coefficient [15]. The R value that relates the calculated results to the target should be very close to one. Thus, an ANN model with the smallest error and the largest correlation coefficient is optimal for prediction. The input layer contains the numbers of input variables and predicted values. The hidden layer consists of neurons, each of which applies a mathematical model to determine the output as a function of the input variable. In the output layer, the result calculated by the analysis is generated [23,24].

In a multilayer perceptron (MLP), a type of ANN model, neurons or connection points are used with a feedforward transmission algorithm between the input and output data. Depending on the nature of the given input parameters, the number of layers is chosen to optimise the network. The MLP algorithm has a changeable structure, and networks may consist of different numbers of neurons and hidden layers. By choosing appropriate weights and transfer functions, smooth, measurable results are obtained between the input and output datasets. In our study, the MLP algorithm and the MATLAB ANN toolbox were used together to train the model on the dataset. By determining the epoch value for which the hidden layers were closest, the MLP could be run again for that number of epochs in the system. The outlet (target) results and the R values for the system by changing the dataset can be obtained via MLP. Fig. 1 illustrates the proposed MLP algorithm, and pseudocode can be found in the Appendix.

3. System and data

Experimental data from a BFBC with a produced power of 0.3 MWe, dimensions of 0.45 × 0.45 × 1 m, and consisting of five modules were used to analyse the temperatures of the combustion chamber and the external surface of the side wall. In the furnace, where Beypazari lignite with low calorific value and a high ash content (with a throughput of 101 kg/h) was used as fuel, temperature measurements were recorded during two combustion tests, with and without recycling. Measurements were made along the height of

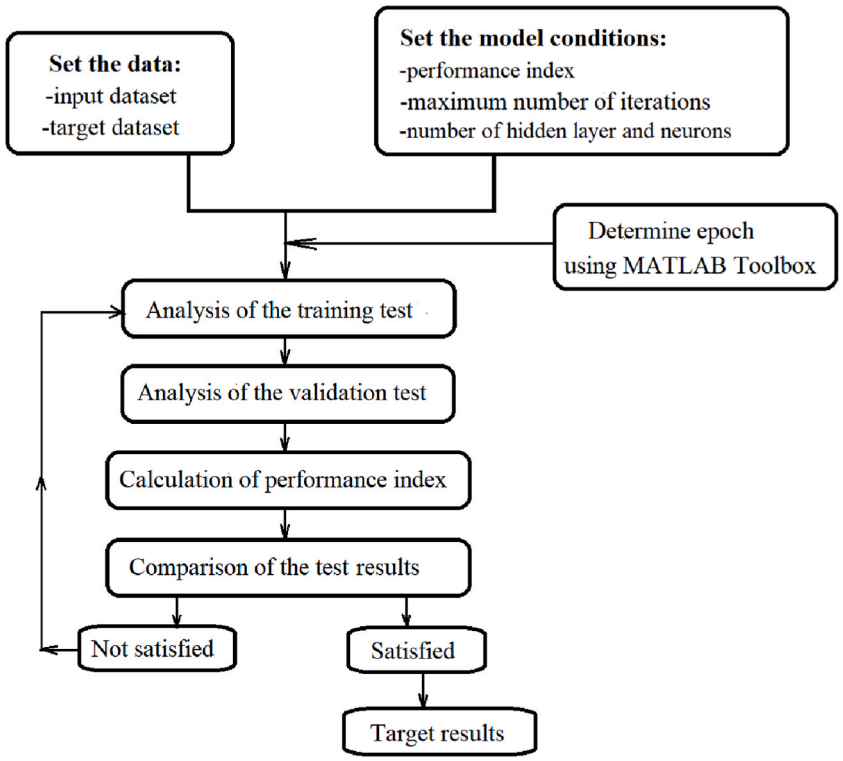


Fig. 1. The proposed MLP algorithm.

the furnace, via thermocouples and radiometers at 14 points on the side wall, to measure the temperature and radiant flux. The amount of coal used in both experiments was the same. In the first experiment, the average bed temperature for the first experiment was ~1150 K and the exit temperature was 1115 K, while in the second experiment, the average bed temperature was ~1107 K and the exit temperature was 1050 K. It was found that the participating gases in the form of CO_2 and H_2O vapour were present in the combustion chamber at a rate of 10%. Detailed information about this system can be found in Refs. [25,26]. The temperature distributions in the medium and at the walls of the furnace, which were arranged according to the measured values, are defined with the following polynomials for the two test operations.

The gas temperature distribution is calculated as follows:

$$T_m(z) = \sum_{i=0}^{6} a_i z^i \tag{3}$$

where the coefficients are:

Test 1 $a_0 = 1149.66$, $a_1 = -15.50$, $a_2 = -1.35$, $a_3 = 42.65$, $a_4 = -30.56$, $a_5 = 7.84$, $a_6 = -0.71$
Test 2 $a_0 = 1106.52$, $a_1 = -16.62$, $a_2 = -90.85$, $a_3 = 116.33$, $a_4 = -50.22$, $a_5 = 9.56$, $a_6 = -0.73$

The wall temperature distribution is calculated as:

$$T_w(z) = \sum_{i=0}^{6} b_i z^i \tag{4}$$

with coefficients:

Test 1 $b_0 = 1146.50$, $b_1 = 40.50$, $b_2 = -129.23$, $b_3 = 137.01$, $b_4 = -62.89$, $b_5 = 13.14$, $b_6 = -1.04$
Test 2 $b_0 = 1110.44$, $b_1 = 61.59$, $b_2 = -226.77$, $b_3 = 246.25$, $b_4 = -106.20$, $b_5 = 20.58$, $b_6 = -1.52$

The absorption properties of the gases (CO_2 and H_2O) in the furnace vary as a function of the medium temperature and the wavelength range. The spectral band model proposed by Bordbar et al. [27] is applied to the gases in the fluidised bed combustion medium, and the expression in Eq. (5) is obtained [26]. Here, P is calculated from the molar concentrations of the gases $PL = (\boldsymbol{X}_{CO2} + \boldsymbol{X}_{H2O})$, and represents the partial pressure of the medium, whereas L is the mean radiation path ($L = 3.6 \times$ *volume/surface area*). In Eq. (5), the j index represents the spectral wide band number.

$$\kappa_{g,j} = a_1 + a_2 \ln(T_m) + a_3 \ln(PL) + a_4 \ln^2(T_m) + a_5 \ln^5(PL) + a_6 \ln(T_m)\ln(PL) \tag{5}$$

The gas absorption properties can be also calculated using the Leckner correlation [27] as an alternative approach:

$$\varepsilon(T, PL_e) = \exp\left\{ a_{ij} + \sum_{j=1}^{M} a_{ij} [\log(PL_e)]^j \right\} \tag{6}$$

where the coefficients a are calculated using the coefficients C_{ij} for the CO_2 and H_2O vapour. The values of the coefficients a and C_{ij} can be found in Ref. [28].

$$a_i = C_{oj} + \sum_{i=1}^{N} C_{ij} \left(\frac{T}{1000} \right)^j \tag{7}$$

In another study related to FBC [7], the enthalpy of the flue gas (h_{gas}) is defined as a quadratic polynomial using the furnace medium

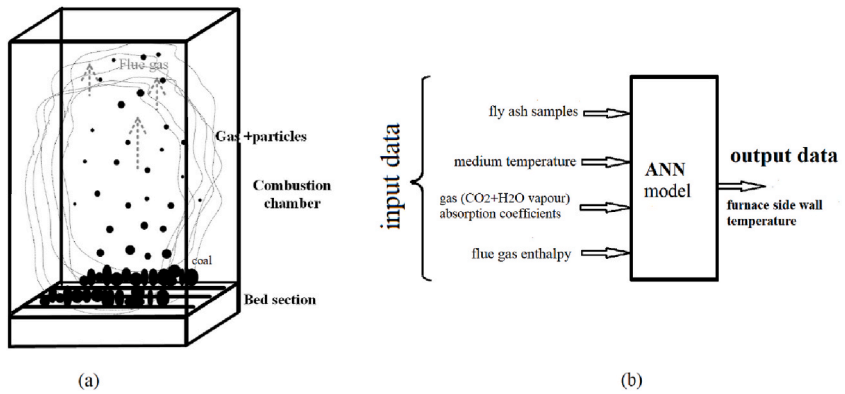


Fig. 2. (a) Schematic diagram of the BFBC and (b) inputs/outputs used in the ANN.

temperature:

$$h_{gas} = a \cdot T_m^2(z) + b \cdot T_m(z) + c \ \left(\mathrm{kJ} \,/\, \mathrm{m}^3\right) \tag{8}$$

with coefficients:

$$a = 1.72546 \times 10^{-5}, b = 0.2336275, c = 18.58662$$

The study in Ref. [9] evaluated the presence of fly ash particles from the types of coal used as fuel and their chemical contents in terms of the absorption coefficient of the combustion production particles, and listed the percentage values for 10 components of fly ash samples from 40 types of coal: SiO_2, Al_2O_3, Fe_2O_3, CaO, MgO, SO_3, K_2O, Na_2O, TiO_2, and P_2O_5. In our analysis, the temperature measurements at the side wall of the furnace were chosen as the output (target) values in order to find the parameters that affect the heat transfer inside the furnace. Fig. 2 shows a schematic diagram of the BFBC chamber and the input and output data for the ANN model. A diagram of the ANN model is shown in Fig. 3.

The minimum and maximum values of the input dataset are given in Table 1.

4. Results and discussion

We analysed the heat transfer in the combustion chamber, the enthalpy of the flue gas, the absorption properties of the CO_2 and H_2O vapour and the components (%) of the fly ash particles in the combustion medium, using two different algorithms based on ANNs. In the first analysis, a backpropagation method was applied to the evaluation of all variables.

The dataset consisted of the medium temperatures ($\mathbf{T_m}$) = (T_m^1, T_m^2, …. …, T_m^z), the fly ash sample components (%), the flue gas enthalpy (h_{gas}) and the gas absorption coefficients $\kappa(z, T, PL)$. A total dataset of 15,410 samples was used as input, including 670 values for the medium temperature, 3350 data points on the percentages of fly ash components, 670 values for the flue gas enthalpy, and 6700 values for the gas absorption coefficients for the 10 bands. The number of data points for the gas absorption coefficients used to calculate the Leckner correlation was 1340. The performance index of the model was set to 10^{-7}, and the maximum number of iterations to 1000. In an analysis of the individual parameters of the system, the correlation coefficients of the different layers, the numbers of neurons and the initial values were determined. Table 2 shows the R values for the different layers and the numbers of neurons for each data input. The results for the training (T), evaluation (E) and test (Tt) phases are given in the form of R values. From our results and from the results in Ref. [29], we see that the number of neurons has an impact on the value of R. From the values in Table 2, a total of 10 hidden layers with 10 neurons was found to be optimal. In application of the backpropagation algorithm, training of the data, analysis and evaluation of the results were performed using the MATLAB R2022b Neural Net Fitting Toolbox with multilayer backpropagation (10 hidden layers), the tansig transfer function, the LM learning algorithm, and 10 neurons in each layer.

Fig. 4 shows the results of the analyses for all datasets using the ANN model. In these analyses, the furnace height was used as the mean radiation path (L) when calculating the gas absorption properties. From the results in Fig. 4, it can be seen that the components of the combustion chamber and the side wall temperature of the furnace are linearly dependent on each other, and the results of the training and test analyses are very close to the experimental data. The correlation coefficient (R) was found to be 0.92241 for the training results and 0.91842 for the testing results. The deviations from the diagonal are random and not systematic. Hence, the generalisation ability of the network model is acceptable for all tests, with target errors of 0.03282.

The fly ash components of the various coal types are random data, which cannot be expressed by a polynomial, and it is not necessary to investigate these components individually. The effects of the fly ash components on the heat transfer in the BFBC chamber were therefore investigated as a whole dataset. Fig. 5 shows the results from this dataset without the percentages of fly ash components.

To investigate the effects of the fly ash content (%) on heat transfer in the combustion chamber, we can compare Figs. 4 and 5 to observe that the R value for the test results for the whole dataset is 0.91183, while the R value for the dataset without the fly ash content (%) is 0.9545. The dataset in the second analysis is modelled with a target error of −2.064. Based on the results of all these

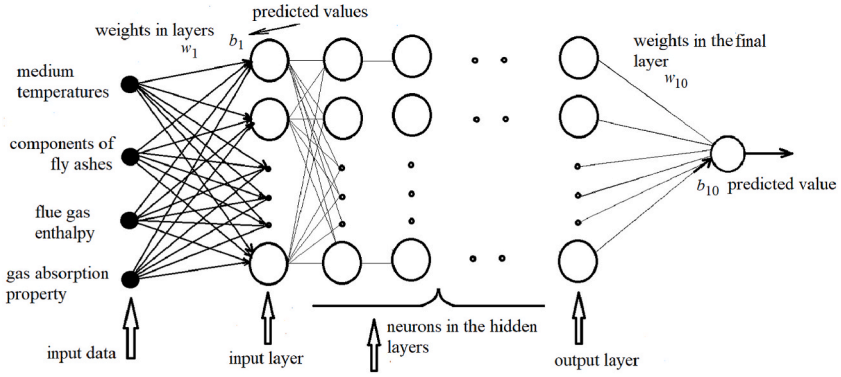


Fig. 3. Schematic representation of the ANN model.

Table 1
Maximum and minimum values in the dataset.

Data		Minimum values	Maximum values
Gas temperature		1050 K	1175 K
Fly ash components (%)	SiO_2	8.20	74.0
	Al_2O_3	5.59	41.20
	Fe_2O_3	0.99	20.93
	CaO	0.16	56.49
	MgO	0.17	9.04
	SO_3	0	31.36
	K_2O	0.27	3.73
	Na_2O	0	2.89
	TiO_2	0.08	2.48
	P_2O_5	0.03	1.95
(CO_2+H_2O vapour) absorption coefficients (m^{-1})		0.24	0.37

Table 2
R values for different numbers of layers and neurons.

Data	Hidden layers	Neurons	Epoch number	*R*
Medium temperature	2	10	100	T: 0.89319; E: 0.90206; Tt: 0.95447
	4	10	100	T: 0.88922; E: 0.91300; Tt: 0.96174
	4	8	345	T: 0.91651; E: 0.86513; Tt: 0.85987
	10	8	183	T: 0.90454; E: 0.89543; Tt: 0.90957
	10	10	990	T: 0.90616; E: 0.91656; Tt: 0.85401
(CO_2+H_2O vapour) absorption coefficient	2	10	116	T: 0.88421; E: 0.84297; Tt: 0.89151
	4	10	188	T: 0.94808; E: 0.89409; Tt: 0.87521
	4	8	129	T: 0.89596; E: 0.89749; Tt: 0.93548
	10	8	153	T: 0.94295; E: 0.91582; Tt: 0.88109
	10	10	849	T: 0.94654; E: 0.88700; Tt: 0.92715
Flue gas enthalpy	2	10	119	T: 0.89581; E: 0.89095; Tt: 0.86627
	4	10	122	T: 0.90388; E: 0.91844; Tt: 0.87013
	4	8	111	T: 0.90676; E: 0.87340; Tt: 0.89483
	10	8	131	T: 0.89090; E: 0.90910; Tt: 0.93942
	10	10	994	T: 0.90241; E: 0.89131; Tt: 0.87426

calculations, it was concluded that the effect of the fly ash component (%) is 4.5%. It was also concluded that the fly ash samples reduced the radiative heat transfer. This inhibitory effect, which is due to the fact that fly ash affects the interaction between oxygen and combustible materials, was also observed in the analysis presented in Ref. [15].

Fig. 6 shows the calculated results from an investigation of the influence of the enthalpy of flue gas containing fly ash particles and other combustion product gases (CO, SO_2, NOx) on the heat transfer of the furnace side wall. The value of the correlation coefficient is $R = 0.99004$ and the error of the target is -0.3713, which confirms the impact of the fly ash content (%) as the results shown in Fig. 5.

When studying the effects of the gas absorption properties on the heat transfer in the combustor, we analysed the absorption properties of the gases (CO_2 and H_2O vapour) based on a value for the mean radiation length of the gas of $L = 0.326$, using the expression reported by Bordbar et al. The results of analyses based on the mean radiation path along the entire length of the combustor were shown in Fig. 4; the results from this stage are presented in Fig. 7, and it can be seen that the *R* value for this analysis is 0.64687 and the target error is 0.9134 when the training, validation and testing phases are included in the calculation process. From a comparison of Figs. 4 and 7 for the two different mean radiation paths ($L = 3.35$ and $L = 0.326$) for the whole dataset, it can be concluded that the mean radiation path strongly influences the heat transfer in the system. In a paper by Johansson et al. [30], who investigated the effects of particle and gas radiation on the total radiative heat transfer in a furnace using a detailed model, it was reported that the total radiation and the gas radiation appear to have similar effects as the length of the furnace and the optical thickness (e.g., *L*) are increased. Our results are consistent with the results of this study [30]. In another study, Chen et al. [31] carried out an experimental investigation of the heat transfer characteristics in a supercritical CFBC, and found that the furnace height had a strong effect on the heat flux distribution in the combustion chamber.

When the gas absorption properties are calculated based on the Leckner correlation, we obtain the radiative properties for the CO_2 and H_2O vapour for only one band. The results are shown in Fig. 8 for both the entire dataset and without the fly ash component percentages, for $L = 3.35$. From Fig. 8(a), it can be seen that the *R* value for the whole system is 0.6455 when the training, validation and testing phases are included in the calculation process, whereas Fig. 8(b) shows that the *R* value for the second case is 0.6822. By comparing the results based on the expression for the gas absorption presented by Bordbar et al. [27] and the expression involving the Leckner correlation [28] (i.e., comparing Figs. 4 and 8(a)), we can see that the effects on the heat transfer of the system are more obvious when the expression for the gas absorption proposed by Bordbar et al. [27] is used. Again, from a comparison of the results with and without the fly ash component percentages (i.e., a comparison of Figs. 5 and 8(b)) based on the gas absorption property, we

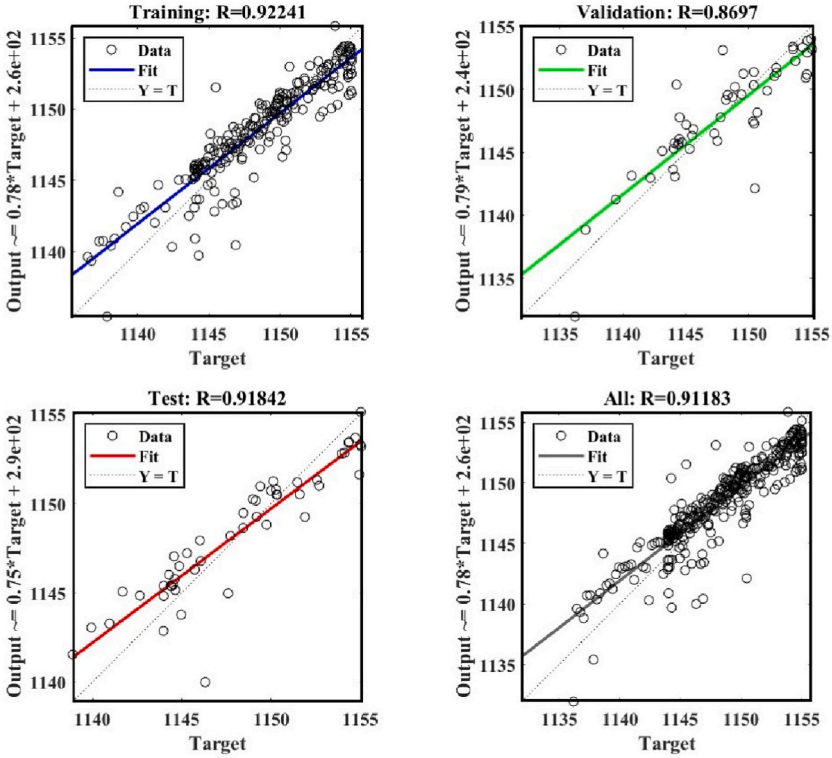


Fig. 4. ANN results for the complete dataset.

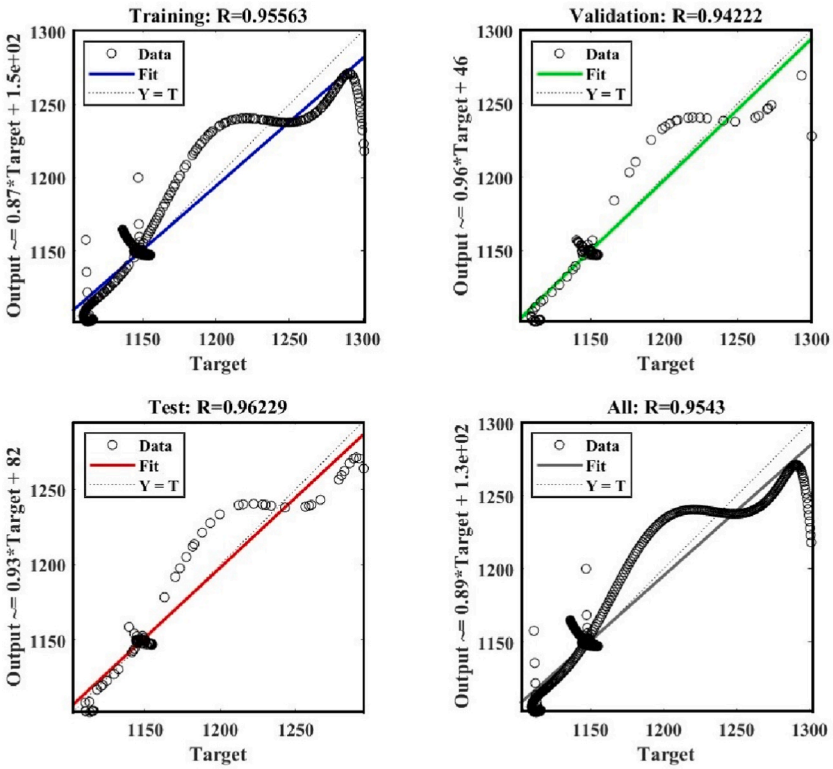


Fig. 5. ANN results for the dataset without the fly ash content (%) of the coal types.

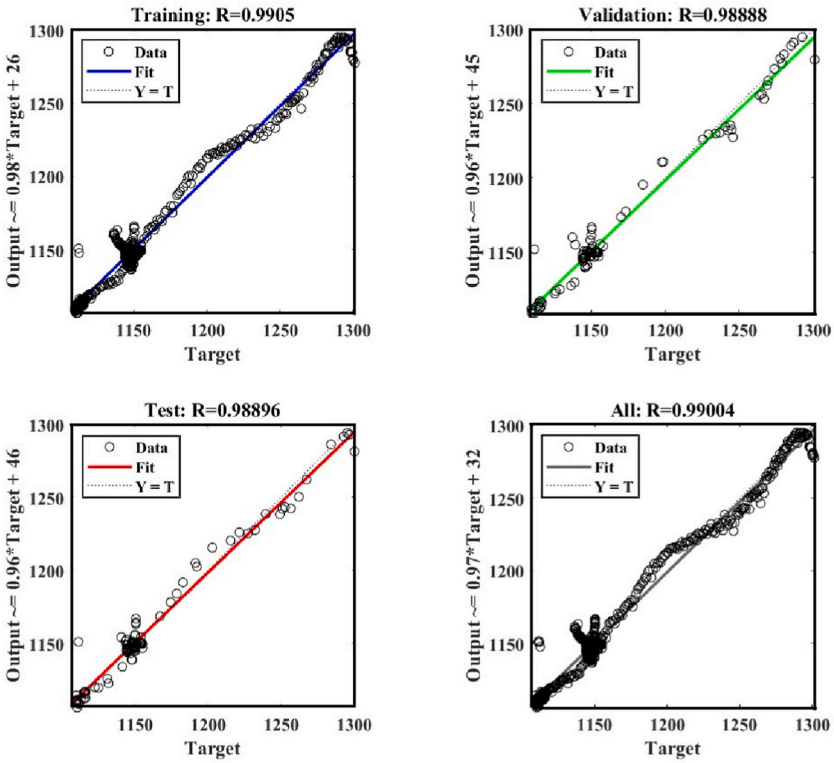


Fig. 6. ANN results for system ($L = 3.35$) without the enthalpy of the flue gas.

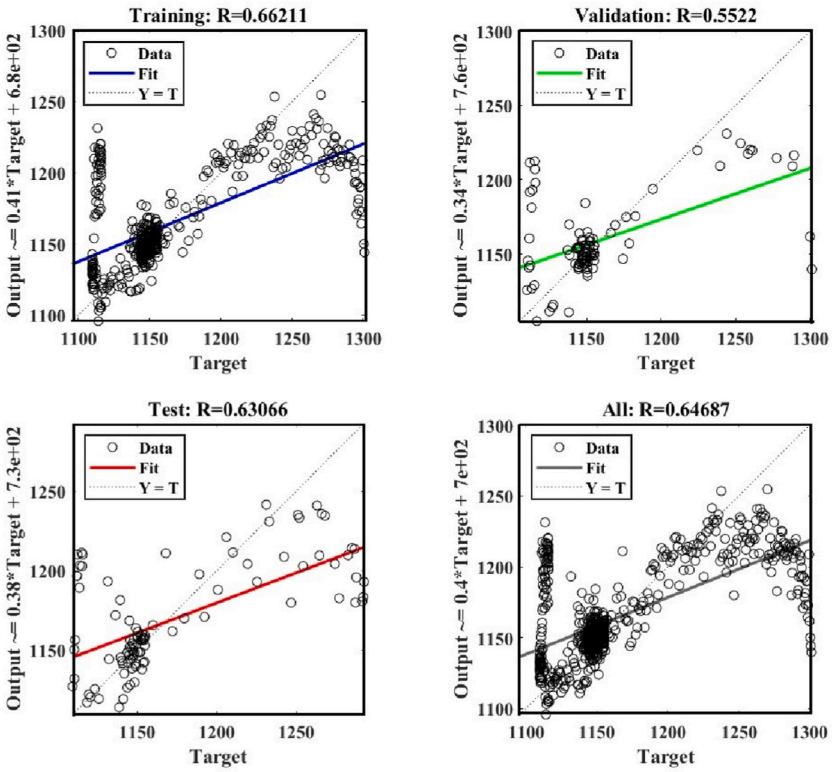


Fig. 7. ANN results for the entire dataset using the system with $L = 0.326$.

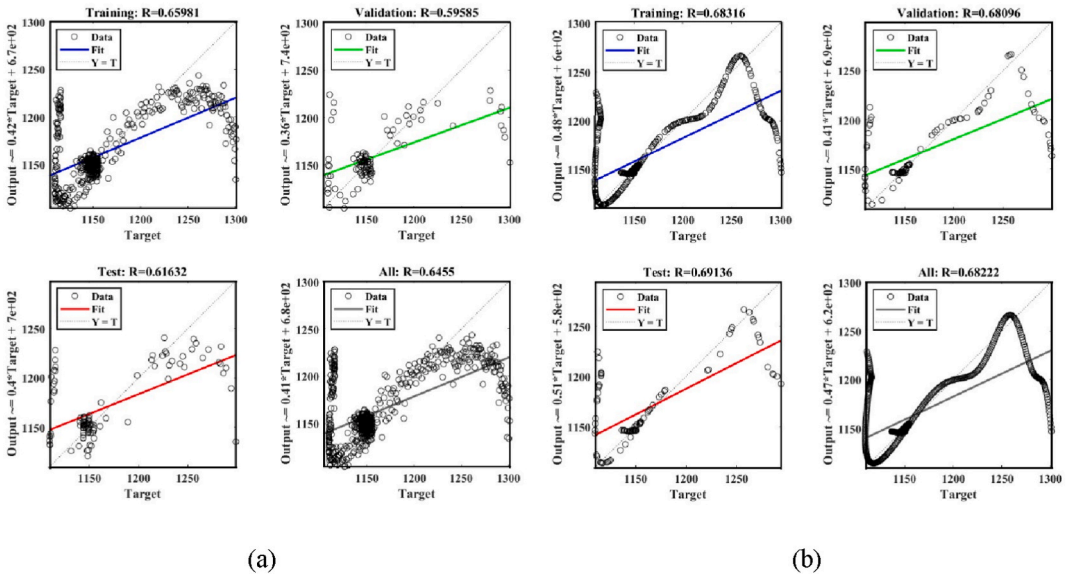


Fig. 8. ANN results for the system using the Leckner correlation for the gas absorption properties ($L = 3.35$): (a) for the whole dataset, and (b) without the percentages of the fly ash components.

find that the R values for all the results presented in Fig. 8(b) are smaller than those in Fig. 5.

In the second phase of our ANN modelling, an MLP algorithm was developed for an investigation of an arbitrary dataset. This algorithm has a different mode of application from the other algorithms in toolbox of the ANN model. An MLP is an application based on artificial intelligence and its accuracy of prediction increases with experience, as mentioned in Ref. [31]. The results of these procedures were an accuracy of approximately 98% and a target error of 0.0968, as shown in Fig. 9.

5. Conclusions

The heat transfer in the combustion chamber of a BFBC system was analysed in terms of the effects of the medium temperature, the flue gas enthalpy, the gas absorption coefficients (for CO_2 and H_2O vapour), and the percentages of fly ash components on the heat transfer. A backpropagation algorithm based on an ANN model with 10 hidden layers and 10 neurons was used, and all the parameters were individually examined in a performance analysis of the training, evaluation, and test stages. The effect of the percentages of fly

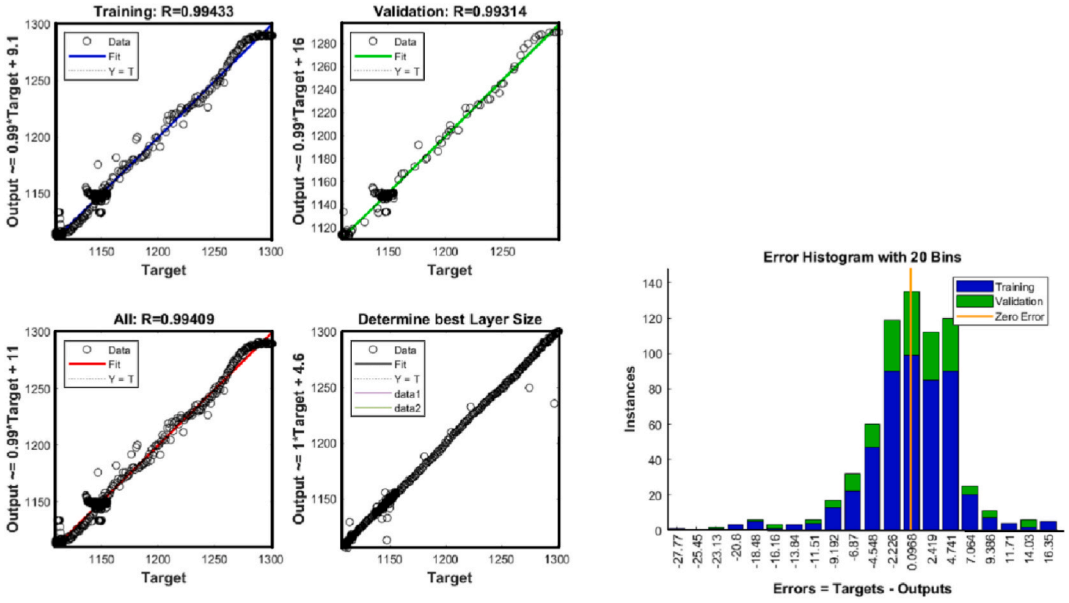


Fig. 9. MLP results for the complete dataset.

ash components on the heat transfer in the combustor was found to be about 4.5% when examined based on Bordbar's expression for the gas absorption, and about 6% when calculated based on the Leckner correlation. The effect of the mean free path (L) on the absorbing gas calculations on the heat transfer in the system was 29.01%. Bordbar's expression for the spectral gas absorption was used to ensure accurate, sensitive heat transfer calculations. The effect of the flue gas enthalpy was 8.6%, and caused a reduction in heat transfer. The proposed MLP algorithm provided highly accurate results, and offers the possibility of investigating different input datasets. Based on the results obtained from this analysis, it was shown that the effects on the heat transfer in the furnace for the given parameter dataset can be determined sensitively and realistically using the ANN model.

Funding

The authors received no financial support for the research.

CRediT authorship contribution statement

Nimeti Doner: Conceptualization, Methodology, Data curation, Writing – original draft, Supervision, Writing – review & editing. **Kerem Ciddi:** Conceptualization, Methodology, Data curation, Writing – original draft, Writing& editing. **Ibrahim Berk Yalcin:** Conceptualization, Methodology, Data curation, Programming. **Muhammed Sarivaz:** Methodology, Data curation, Programming.

Declaration of competing interest

The authors declare that they have no known competing financial interests or personal relationships that could have appeared to influence the work reported in this paper.

Data availability

The data that has been used is confidential.

Appendix A. Supplementary data

Supplementary data to this article can be found online at https://doi.org/10.1016/j.csite.2023.103145.

References

[1] H. Harmandar, Effect of recycling on the performance of bubbling fluidized bed combustors, in: Master of Science Thesis, Middle East Technical University, Ankara, June 2003.
[2] Y. Lv, F. Hong, T. Yang, F. Fang, J. Liu, A dynamic model for the bed temperature prediction of circulating fluidized bed boilers based on least squares support vector machine with real operational data, Energy 124 (2017) 284–294.
[3] D.E. Alagoz, Mathematical Modeling of Fluidized Bed Combustors with Radiation Model, Master of Science Thesis, Middle East Technical University (METU), Ankara, 2006.
[4] M. Zahedi, F. Rajabipour, Fluidized bed combustion (FBC) fly ash and its performance in concrete, ACI Mater. J. 116 (4) (2019).
[5] G. Yue, J. Lu, H. Zhang, H. Yang, J. Zhang, Q. Liu, Z. Li, E. Joos, P. Jaud, Design Theory of Circulating Fluidized Bed Boilers. 18th International Conference on Fluidized Bed Combustion, 2005.
[6] S.A. Kalogirou, Artificial intelligence for the modeling and control of combustion processes: a review, Prog. Energy Combust. Sci. 29 (2003) 515–566.
[7] H. Zhou, K. Cen, J. Fan, Multi-objective optimization of the coal combustion performance with artificial neural networks and genetic algorithms, Int. J. Energy Res. 29 (2005) 499–510.
[8] J.S. Chandok, I.N. Kar, S. Tuli, Estimation of furnace exit gas temperature (FEGT) using optimized radial basis and back-propagation neural networks, Energy Convers. Manag. 49 (2008) 1989–1998.
[9] J. Krzywanski, W. Nowak, Modeling of heat transfer coefficient in the furnace of CFB boilers by artificial neural network approach, Int. J. Heat Mass Tran. 55 (2012) 4246–4253.
[10] D. Li, Q. Deng, D. Lee, C.H. Jeon, Prediction of attrition rate of coal ash for fluidized bed based on chemical composition with an artificial neural network model, Fuel Process. Technol. 225 (2022), 107024.
[11] M. Liukkonen, M. Heikkinen, T. Hiltunen, E. Hälikkä, R. Kuivalainen, Y. Hiltunen, Artificial neural networks for analysis of process states in fluidized bed combustion, Energy 36 (2011) 339–347.
[12] H. Zhong, Z. Sun, J. Zhu, C. Zhang, Prediction of solid holdup in a gas–solid circulating fluidized bed riser by artificial neural networks, Ind. Eng. Chem. Res. 60 (8) (2021) 3452–3462.
[13] H. Yu, M. Gao, H. Zhang, Y. Chen, Dynamic modeling for SO2-NOx emission concentration of circulating fluidized bed units based on quantum genetic algorithm - extreme learning machine, J. Clean. Prod. 324 (2021), 129170.
[14] D. Serrano, D. Castelló, Tar prediction in bubbling fluidized bed gasification through artificial neural networks, Chem. Eng. J. 402 (2020), 126229.
[15] H. Bi, C. Wang, Q. Lin, X. Jiang, C. Jiang, L. Bao, Combustion behavior, kinetics, gas emission characteristics and artificial neural network modeling of coal gangue and biomass via TGFTIR, Energy 213 (2020) 118290.
[16] J.M. Zurada, in: St Paul (Ed.), Introduction to Artificial Neural Systems, MN, West Publishing Company, 1992.
[17] S. Haykin, Neural Networks and Learning Machines, third ed., Pearson Education Inc, Upper Saddle River, New Jersey, 2009.
[18] K. Lou, J. Xing, Y. Bai, J. Fan, Prediction of product distributions in coal devolatilization by an artificial neural network model, Combust. Flame 193 (2018) 283–294.
[19] A. De Lucas, A. Duran, R. Carmona, M. Lapuerta, Modeling diesel particulate emissions with neural networks, Fuel 80 (2001) 539.
[20] A. Duran, A. De Lucas, M. Carmona, R. Ballesteros, Simulation of atmospheric PAH emissions from diesel engines, Chemosphere 44 (2001) 921.
[21] A. Subaşı, K. Erdem, Prediction of specific heat of hybrid nanofluids using artificial neural networks, Journal of the Faculty of Engineering and Architecture of Gazi University 37 (1) (2022) 377–387.

[22] D.S. Pandey, S. Das, I. Pan, J.J. Leahy, W. Kwapinski, Artificial neural network based modelling approach for municipal solid waste gasification in a fluidezed bed reactor, Waste Manag. 58 (2016) 202–213.
[23] M. Upadhyay, V.M. Nagulapati, H. Lim, Hybrid CFD-neural networks technique to predict circulating fluidized bed reactor riser hydrodynamics, J. Clean. Prod. 337 (2022), 130490.
[24] T. Bekat, M. Erdogan, F. Inal, A. Genc, Prediction of the bottom ash formed in a coal-fired power plant using artificial neural networks, Energy 45 (2012) 882–887.
[25] N. Doner, N. Selçuk, An application of Spectral line-based weighted sum of grey gases (SLW) model with geometric optics approximation for radiative heat transfer in 3-D participating media, Appl. Therm. Eng. 50 (1) (2013) 89–93.
[26] M.S. Yasar, G. Ozen, N. Selçuk, G. Kulah, Assessment of improved banded model for spectral thermal radiation in presence of non-gray particles in fluidized bed combustors, Appl. Therm. Eng. 176 (2020), 115322.
[27] H. Bordbar, A. Maximov, T. Hyppänen, Improved banded method for spectral thermal radiation in participating media with spectrally dependent wall emittance, Appl. Energy 235 (2019) 1090–1105.
[28] Howell J.R., Siegel R., Mengüç M.P., Thermal Radiation Heat Transfer fifth ed., CRC Press, Taylor & Francis Group New York.
[29] S. Bhattacharyya, D. Sarkar, R. Roy, S. Chakraborty, V. Goel, E. Almatrafi, Application of new artificial neural network to predict heat transfer and thermal performance of a solar air-heater tube, Sustainability 13 (2021) 7477.
[30] R. Johansson, B. Leckner, K. Andersson, F. Johnsson, Influence of particle and gas radiation in oxy-fuel combustion, Int. J. Heat Mass Tran. 65 (2013) 143–152.
[31] Y. Chen, X. Lu, W. Zhang, Q. Wang, S. Chen, J. Xu, J. Li, Experimental study on the heat-transfer characteristics of a 600 MW supercritical circulating fluidized bed boiler, Energy Fuels 32 (1) (2017) 1–9.